

# Amplitude Equations and Chemical Reaction-Diffusion Systems

M. Ipsen    F. Hynne    P. G. Sørensen

June 20, 2018

*Department of Chemistry, University of Copenhagen, H.C. Ørsted Institutet, Universitetsparken  
5, 2100 DK-Copenhagen, Denmark.*

## Abstract

The paper discusses the use of amplitude equations to describe the spatio-temporal dynamics of a chemical reaction-diffusion system based on an Oregonator model of the Belousov-Zhabotinsky reaction. Sufficiently close to a supercritical Hopf bifurcation the reaction-diffusion equation can be approximated by a complex Ginzburg-Landau equation with parameters determined by the original equation at the point of operation considered. We illustrate the validity of this reduction by comparing numerical spiral wave solutions to the Oregonator reaction-diffusion equation with the corresponding solutions to the complex Ginzburg-Landau equation at finite distances from the bifurcation point. We also compare the solutions at a bifurcation point where the systems develop spatio-temporal chaos. We show that the complex Ginzburg-Landau equation represents the dynamical behavior of the reaction-diffusion equation remarkably well sufficiently far from the bifurcation point for experimental applications to be feasible.

# 1 Introduction

During the last two decades, the study of spiral waves and spatio-temporal chaos in physical, chemical, and biological systems has received much attention. In physics, spiral patterns have been studied extensively in hydrodynamic systems [Cross & Hohenberg 1993]. Recently, spiral formation has also been studied in liquid crystals [Couillet *et al.* 1994]. Biological examples include the growth of the slime mold *Dictyostelium discoideum* [Newell 1983] and potential differences occurring on the surface of rabbit heart muscles [Allesie *et al.* 1977]. In chemical systems, spiral formation and related phenomena like target wave propagation often occur in oscillatory chemical reactions which take place in unstirred media (*e.g.* a petri dish). In this case the spirals appear as concentration variations over the spatial domain of the system. A well-known example of a chemical reaction exhibiting such phenomena, is the Belousov-Zhabotinsky reaction, whose properties in spatially distributed media has been discussed extensively in the chemical literature. For further reference, see Zhabotinsky [1991] and references therein. Recently, observations of spiral wave development and spatio-temporally chaotic patterns close to a supercritical Hopf bifurcation was reported by Ouyang & Flesselles [1996].

The state space of chemical systems exhibiting wave and spatio-temporally chaotic phenomena almost always have a fairly high dimension. Consequently, realistic modeling of such phenomena by direct integration of the reaction-diffusion equation is difficult or sometimes even impossible. For this reason most works in this field have used simplified two-dimensional models, often describing excitable media.

For oscillatory systems, the motion in the concentration space largely takes place on a two-dimensional manifold. In particular, this condition applies near a supercritical Hopf bifurcation where, furthermore, the motion in the plane of oscillations can be described analytically to a very good approximation. Integrating the reaction-diffusion system close to a supercritical Hopf bifurcation can be a very time consuming and difficult task even on a large computer. For this reason, it is of great importance to introduce techniques that utilize the characteristics of the Hopf bifurcation in order to simplify the reaction-diffusion equation (RDE) without changing the essential properties of the solution. As shown by Kuramoto [1984], such a description is offered by the complex Ginzburg-Landau equation (CGLE) which provides a systematic description of the chemical waves near a Hopf bifurcation (of the corresponding homogeneous system). He applied it to the Brusselator, a two-dimensional model for an abstract chemical system.

The CGLE is an amplitude equation which describes the waves of the reaction-diffusion system in terms of a complex amplitude. It offers a number of advantages in addition to a reduction of the effective dimension of the original reaction-diffusion equation. It provides an intuitively natural description of oscillations which facilitates interpretations of results and, furthermore, introduces a scaling which makes it universal, depending only on two complex parameters but not *e.g.* on the distance from the bifurcation point. The scaling also solves a serious problem associated with the integration of reaction-diffusion equations, due to the critical slowing down of the motion in the concentration space which occurs near the bifurcation point. The description becomes increasingly precise as the Hopf bifurcation point is approached and is “exact” in the limit.

As one moves further away from the bifurcation point the CGLE description gradually becomes less precise. Hence we wish to discuss how well the CGLE description approximates realistic reaction-diffusion systems representing actual chemical systems at finite distances from a Hopf bifurcation. This point is very important from an experimental point of view, since experimental observations of waves and spatio-temporal chaos require sufficiently large amplitudes and rates of development for spatial patterns.

The behavior of amplitude equations that apply close to a Hopf bifurcation have for example been studied by Huber *et al.* [1992], Aranson *et al.* [1993], and Nicolis [1995]. However, to our knowledge, there have been no attempts to test how well the CGLE actually does approximate the behavior of a realistic reaction-diffusion system close to a supercritical Hopf bifurcation. By comparing results from simulations of a specific reaction-diffusion system with those of the associated CGLE, we show in this paper that the CGLE indeed gives a very satisfactory description of the original system. We focus attention on two specific conditions for an Oregonator model, where spiral patterns and chaotic patterns can occur when the corresponding homogeneous systems exhibits simple oscillations with small amplitude.

## 2 Review of Theory

We consider a chemical reaction with  $n$  chemical components taking place under heterogeneous conditions described by the reaction-diffusion equation. The reaction-diffusion equation is defined by the rate expression and the diffusion matrix associated with the chemical system under consideration. Let the vector  $\mathbf{c}$  describe the concentrations of the  $n$  dynamical species that participate in the reaction-diffusion system. The associated reaction-diffusion equation can then be written as

$$\dot{\mathbf{c}} = \mathbf{f}(\mathbf{c}; \mu) + \mathbf{D} \cdot \nabla_{\mathbf{r}}^2 \mathbf{c}, \quad (1)$$

where  $\mathbf{f}$  is the rate expression and  $\mathbf{D}$  is the diffusion matrix. Here  $\mu$  designates some controllable parameter which can be varied experimentally and serves as a bifurcation parameter. Assume that this system has a homogeneous and stationary solution  $\mathbf{c}_s$ . The dynamics of small perturbations  $\mathbf{u}(t, \mathbf{r}; \mu) = \mathbf{c}(t, \mathbf{r}; \mu) - \mathbf{c}_s(t; \mu)$  of the stationary point can then be described through a Taylor expansion of the right-hand side of Eq. (1) by

$$\dot{\mathbf{u}} = \mathbf{J} \cdot \mathbf{u} + \frac{1}{2!} \mathbf{M} : \mathbf{u} \mathbf{u} + \frac{1}{3!} \mathbf{N} : \mathbf{u} \mathbf{u} \mathbf{u} + \dots + \mathbf{D} \cdot \nabla_{\mathbf{r}}^2 \mathbf{u}. \quad (2)$$

The matrix  $J_{ij} = \frac{\partial f_i}{\partial c_j}$  is the Jacobian matrix, whereas  $\mathbf{M} : \mathbf{u} \mathbf{u}$  and  $\mathbf{N} : \mathbf{u} \mathbf{u} \mathbf{u}$  denote quadratic and cubic forms in  $\mathbf{u}$ , respectively defined by

$$(\mathbf{M} : \mathbf{u} \mathbf{u})_i = \sum_{j,k=1}^n \frac{\partial^2 f_i}{\partial c_j \partial c_k} \Big|_{\mathbf{c}_s} u_j u_k, \quad (3a)$$

$$(\mathbf{N} : \mathbf{u} \mathbf{u} \mathbf{u})_i = \sum_{j,k,l=1}^n \frac{\partial^3 f_i}{\partial c_j \partial c_k \partial c_l} \Big|_{\mathbf{c}_s} u_j u_k u_l. \quad (3b)$$

$\mathbf{M}$  is often referred to as the Hessian. The stability of the stationary state  $\mathbf{c}_s$  to space-independent perturbations is determined by the eigenvalues of the Jacobian matrix associated with the linearization of the rate expression  $\mathbf{f}(\mathbf{c}; \mu)$  in Eq. (1) around  $\mathbf{c}_s$ . In general, a bifurcation or loss of stability will occur if the real part of one or more of these eigenvalues change sign from negative to positive. Let us assume that  $\mathbf{c}_s$  loses stability via a supercritical Hopf bifurcation at  $\mu = \mu_0$  due to a change of sign in the real part of a complex eigenvalue  $\lambda = \sigma + i\omega$  and its complex conjugate. At the bifurcation point, the eigenvalue  $\lambda$  will therefore be purely imaginary,  $i\omega_0$ . In the homogeneous system, this bifurcation gives rise to small sinusoidal oscillations of the concentrations. In the limit  $\mu \rightarrow \mu_0$ , the frequency of the oscillations will approach the value  $\omega_0$  corresponding to the imaginary part of  $\lambda$  at the bifurcation point.

The equations related to the Hopf bifurcation can be expanded in a formal parameter  $\epsilon$  which often is related to the amplitude of the oscillations. The quantities  $\mathbf{u}$ ,  $\mathbf{J}(\mu)$ ,  $\mathbf{M}(\mu)$ ,  $\mathbf{N}(\mu)$ ,  $\lambda(\mu) = \sigma(\mu) + i\omega(\mu)$  and the original parameter  $\mu$  can be expanded as follows

$$\begin{aligned}\mathbf{u} &= \epsilon\mathbf{u}_1 + \epsilon^2\mathbf{u}_2 + \epsilon^3\mathbf{u}_3 \dots, & \mathbf{J} &= \mathbf{J}_0 + \epsilon^2\mathbf{J}_2 + \epsilon^4\mathbf{J}_4 \dots, \\ \mathbf{M} &= \mathbf{M}_0 + \epsilon^2\mathbf{M}_2 + \epsilon^4\mathbf{M}_4 \dots, & \mathbf{N} &= \mathbf{N}_0 + \epsilon^2\mathbf{N}_2 + \epsilon^4\mathbf{N}_4 \dots, \\ & & \lambda &= \lambda_0 + \epsilon^2\lambda_2 + \epsilon^4\lambda_4 \dots, \\ & & \mu &= \mu_0 + \epsilon^2\mu_2 + \epsilon^4\mu_4 \dots\end{aligned}\quad (4)$$

where  $\lambda_j = \sigma_j + i\omega_j$ ,  $j = 0, 2, 4, \dots$ . The parameter  $\epsilon$  can be defined in many ways. In experimental situations where the bifurcation parameter is a real physical quantity, it is often convenient to choose  $\epsilon$  in a dimensionless form and eliminate it from all expressions that are used to interpret results [Kosek *et al.* 1994].

Consider the behavior of the system in states that locally are close to the homogeneous oscillatory solution. One can prove [Kuramoto 1984] that close to the Hopf bifurcation point the dynamics of the  $n$  chemical species  $\mathbf{c}(t, \mathbf{r}; \mu)$  can be approximated by the following equation

$$\mathbf{c}(t, \mathbf{r}; \mu) = \mathbf{c}_s + \epsilon \left( W(\tau, \mathbf{s}) e^{i\omega_0 t} \mathbf{U}_+ + \overline{W}(\tau, \mathbf{s}) e^{-i\omega_0 t} \overline{\mathbf{U}}_+ \right). \quad (5)$$

Here  $\mathbf{U}_+$  is the complex right eigenvector associated with the bifurcating eigenvalue  $i\omega_0$  at the bifurcation point  $\epsilon = 0$  ( $\mu = \mu_0$ ). The complex amplitude  $W(\tau, \mathbf{s})$  of Eq. (5) must satisfy the complex Ginzburg-Landau equation

$$\frac{\partial W}{\partial \tau} = \lambda_2 W - g|W|^2 W + d\nabla_{\mathbf{s}}^2 W, \quad (6)$$

which depends on  $t$ ,  $\mathbf{r}$ , and  $\epsilon$  through the time and space variables  $\tau$  and  $\mathbf{s}$ , scaled with  $\epsilon$  as  $\tau = \epsilon^2 t$  and  $\mathbf{s} = \epsilon \mathbf{r}$ . One purpose of the scaling is to obtain a description that is independent of the distance from the bifurcation point (as long as the approximation is applicable). The use of the scaled time  $\tau$  solves the problem of critical slowing down exhibited when the system approaches the bifurcation point. In other words, the closer we get to the bifurcation point, the longer the transient time for pattern development. As we shall see, this fact can indeed cause difficulties in numerical studies of the original reaction-diffusion equation, which are absent when the CGLE is used.

The complex parameter  $d$  in the CGLE is determined by the equation

$$d = \mathbf{U}_+^* \cdot \mathbf{D} \cdot \mathbf{U}_+, \quad (7)$$

where  $\mathbf{U}_+^*$  is the left eigenvector corresponding to the bifurcating eigenvalue  $i\omega_0$  at the bifurcation point. The left eigenvector  $\mathbf{U}_+^*$  has been normalized to fulfil the relation  $\mathbf{U}_+^* \cdot \mathbf{U}_+ = 1$ . To find the complex coefficient  $g$  one first determines two vectors  $\mathbf{F}_{20}$  and  $\mathbf{F}_{11}$  by solving the two linear equations [Kuramoto 1984]

$$(\mathbf{J}_0 - 2i\omega_0 \mathbf{I}) \cdot \mathbf{F}_{20} = -\frac{1}{2} \mathbf{M}_0 : \mathbf{U}_+ \mathbf{U}_+, \quad (8a)$$

$$\mathbf{J}_0 \cdot \mathbf{F}_{11} = -\mathbf{M}_0 : \mathbf{U}_+ \overline{\mathbf{U}}_+. \quad (8b)$$

The complex parameter  $g$  can be found by the expression [Kuramoto 1984]

$$g = -\mathbf{U}_+^* \cdot \mathbf{M}_0 : \mathbf{U}_+ \mathbf{F}_{11} - \mathbf{U}_+^* \cdot \mathbf{M}_0 : \overline{\mathbf{U}}_+ \mathbf{F}_{20} - \frac{1}{2} \mathbf{U}_+^* \cdot \mathbf{N}_0 : \mathbf{U}_+ \mathbf{U}_+ \overline{\mathbf{U}}_+. \quad (9)$$

In Eq. (8) and Eq. (9), the tensors  $\mathbf{J}_0$ ,  $\mathbf{M}_0$ , and  $\mathbf{N}_0$  denote the values of  $\mathbf{J}$ ,  $\mathbf{M}$ , and  $\mathbf{N}$  at the bifurcation point  $\mu = \mu_0$ .

The complex Ginzburg-Landau equation is often presented in the form

$$\frac{\partial W}{\partial \tau} = W - (1 + i\beta)|W|^2W + (1 + i\alpha)\nabla_{\mathbf{s}}^2W. \quad (10)$$

Here  $\alpha = \frac{d''}{d'}$  and  $\beta = \frac{g''}{g'}$ , where  $d' = \text{Re } d$ ,  $d'' = \text{Im } d$ ,  $g' = \text{Re } g$ , and  $g'' = \text{Im } g$ . One obtains this dimensionless version of the complex Ginzburg-Landau equation by performing the variable change  $\tau \rightarrow \sigma_2^{-1}\tau$ ,  $\mathbf{s} \rightarrow \sqrt{\frac{d'}{\sigma_2}}\mathbf{s}$ ,  $W \rightarrow \sqrt{\frac{\sigma_2}{|g'|}}\exp(i\frac{\omega_2}{\sigma_2}\tau)$ .

One can easily show that in a one-dimensional spatial domain of infinite length Eq. (10) admits of plane wave solutions of the form

$$W_Q(x, t) = R_Q e^{i(Qx - \omega_Q t)}, \quad (11)$$

where the frequency  $\omega_Q$  and amplitude  $R_Q$  have to satisfy the relations

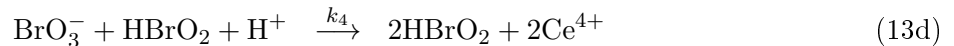
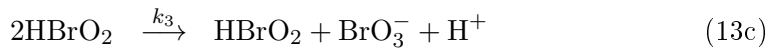
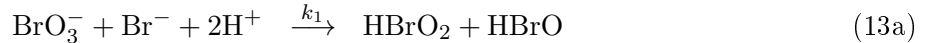
$$R_Q = \sqrt{1 - Q^2}, \quad |Q| < 1, \quad (12a)$$

$$\omega_Q = \beta Q^2 + \alpha(1 - Q^2). \quad (12b)$$

By considering perturbations of the plane wave solutions, one can prove that these become unstable when  $\alpha$  and  $\beta$  satisfy the relation  $1 + \alpha\beta < 0$ . The quantity  $1 + \alpha\beta = 0$  determines the boundary of the Benjamin-Feir instability which is associated with spatio-temporally chaotic behavior in the system. Since spiral wave solutions far from the spiral core asymptotically approach a plane wave locally, one would expect that crossing the boundary of the Benjamin-Feir instability also implies a breakdown of spiral waves and perhaps development of chaotic behavior. In Sec. 4 we shall present examples showing the breakdown of spiral wave solutions in both the reaction-diffusion equation and the Ginzburg-Landau equation.

### 3 Model description

As a model for a real chemical system we have chosen the three dimensional Oregonator [Field & Noyes 1974]. The Oregonator is based on the so-called FKN-mechanism, which provided the first successful explanation of the chemical oscillations that occur in the BZ-reaction [Field *et al.* 1972]. During the last two decades, the Oregonator model has been modified in many ways by inclusion of additional chemical reaction steps or by changing the rate constants. The model used in this study consists of the original Oregonator mechanism



with rate constants  $k_1, \dots, k_5$  from Field & Försterling [1986]. The quantity  $f$  is a stoichiometric factor. For notational simplicity we introduce  $A = [\text{BrO}_3^-]$ ,  $H = [\text{H}^+]$ ,  $X = [\text{HBrO}_2]$ ,  $Y = [\text{Br}^-]$ , and  $Z = [\text{Ce}^{4+}]$ , where  $[S]$  is the concentration of species  $S$ . For relevant experimental conditions

we may assume that  $[\text{BrO}_3^-]$  and  $[\text{H}^+]$  are constant. By applying mass law kinetics, the time and space variation of the spatially distributed Oregonator model can be described by the following three coupled partial differential equations

$$\frac{\partial X}{\partial t} = k_1 A H^2 Y - k_2 H X Y - 2k_3 X^2 + k_4 A H X + D_X \nabla_{\mathbf{r}}^2 X, \quad (14a)$$

$$\frac{\partial Y}{\partial t} = -k_1 A H^2 Y - k_2 H X Y + k_5 f Z + D_Y \nabla_{\mathbf{r}}^2 Y, \quad (14b)$$

$$\frac{\partial Z}{\partial t} = 2k_4 A H X - k_5 Z + D_Z \nabla_{\mathbf{r}}^2 Z, \quad (14c)$$

where  $D_X$ ,  $D_Y$ , and  $D_Z$  are the diffusion constants of the species  $\text{HBrO}_2$ ,  $\text{Br}^-$ , and  $\text{Ce}^{4+}$  respectively (for dilute solutions, the diffusion matrix is diagonal to a good approximation). For a thorough discussion of the chemistry on which the Oregonator is based, the reader is referred to Tyson [1985]. The values of the stoichiometric factor  $f$  [Nielsen *et al.* 1991], of the rate constants and of the diffusion constants used in the numerical studies are shown in table 1. For the diffusion constants, we have used estimates by Hynne & Sørensen [1993].

## 4 Numerical simulations

The parameters  $\alpha$  and  $\beta$  in Eq. (10) have a complicated functional dependence on the parameters that characterize the Hopf bifurcation in the original reaction-diffusion system as is evident from Eqs. (7)–(9). If a parameter in the original model system is changed slightly, a new Hopf bifurcation can be found by adjusting another parameter, corresponding to the fact that the Hopf bifurcation is a generic co-dimension one bifurcation. The Ginzburg-Landau parameters  $\alpha$  and  $\beta$  will also change due to Eqs. (7) and (9). It is therefore convenient to study the variation of the parameters  $\alpha$  and  $\beta$  along a branch in a Hopf bifurcation diagram where the Hopf bifurcation is continued as a function of two appropriate parameters in the particular system. For the present Oregonator model, we have chosen the concentrations of  $\text{BrO}_3^-$  and  $\text{H}^+$  as bifurcation parameters, since these easily can be varied experimentally and are almost constant during an experiment. The bifurcation diagram obtained for the Oregonator model is shown in Fig. 1. The curve consists of two branches representing super- and subcritical Hopf bifurcations shown as the solid and dashed parts of the curve in Fig. 1. This change of stability occurs at  $[\text{BrO}_3^-] = 0.269 \text{ M}$  and  $[\text{H}^+] = 0.176 \text{ M}$  ( $\text{M} = \text{mol dm}^{-3}$ ).

Since Eq. (6) applies to a supercritical Hopf bifurcation only, our attention will be limited to the supercritical branch in the bifurcation diagram. One can calculate the parameters  $\alpha$  and  $\beta$  from Eqs. (7) and (9) along the bifurcation curve plotted as functions of  $[\text{BrO}_3^-]$  in Fig. 2. We see that the diffusion parameter  $\alpha$  changes slightly as the Hopf bifurcation point varies with the bifurcation parameters  $[\text{BrO}_3^-]$  and  $[\text{H}^+]$ . This variation is due to the fact that the directions of the right and left eigenvectors of the Jacobian matrix  $\mathbf{J}_0$  change with the Hopf bifurcation point. The coefficient  $\beta$  shows a more dramatic change along the bifurcation curve. At the right-hand edge of the supercritical branch,  $\beta$  diverges to infinity because the denominator of  $\beta = \frac{g'}{g}$  becomes zero at the transition from supercritical to subcritical behavior. An extended Ginzburg-Landau approach may still apply close to the singularity if a quintic term is added to the complex Ginzburg-Landau equation. However, this modification will not be considered in this paper.

A crucial term which can be calculated from the values of  $\alpha$  and  $\beta$  along the Hopf bifurcation branch is the Benjamin-Feir parameter  $1 + \alpha\beta$ , which determines whether plane waves

are unstable ( $1 + \alpha\beta < 0$ ) to small perturbations in one space dimension. The variation of  $1 + \alpha\beta$  along the supercritical part of the Hopf bifurcation curve is exhibited in Fig. 3 which shows that a Benjamin-Feir instability starts at  $[\text{BrO}_3^-]_{\text{BF}} = 0.073 \text{ M}$  and  $[\text{H}^+]_{\text{BF}} = 0.348 \text{ M}$ . For  $[\text{BrO}_3^-] < [\text{BrO}_3^-]_{\text{BF}}$  and  $[\text{H}^+] > [\text{H}^+]_{\text{BF}}$ , we may therefore expect to find stable spiral wave solutions to the reaction-diffusion system as well as to the complex Ginzburg-Landau equation. Spiral waves are expected to become unstable when  $[\text{BrO}_3^-] > [\text{BrO}_3^-]_{\text{BF}}$  and  $[\text{H}^+] < [\text{H}^+]_{\text{BF}}$ . (Recall that  $[\text{BrO}_3^-]$  and  $[\text{H}^+]$  vary together on the Hopf bifurcation curve.)

We have selected two points on the (supercritical) Hopf bifurcation curve for comparisons of the (Oregonator based) reaction-diffusion system with the corresponding complex Ginzburg-Landau equation as indicated on Fig. 1. The characteristic Ginzburg-Landau parameters for the two points are shown in table 2. The points differ in the sign of the Benjamin-Feir parameter,  $1 + \alpha\beta$ ; they are marked on Fig. 3. The complex Ginzburg-Landau equation applies near a Hopf bifurcation and is scaled so that its form is independent of the distance from the bifurcation point. Thus,  $\alpha$  and  $\beta$  are defined at the bifurcation. However, we want to compare solutions to the complex Ginzburg-Landau equation which is independent of the distance from the bifurcation point with those of the reaction-diffusion system for which the distance from the bifurcation point is important. In the latter case, one must work at definite (finite) distances from the bifurcation curve. The points are chosen with the following considerations in mind: If a point is too close to the bifurcation curve, significant spatial changes in amplitude take so long (compared to a local period of oscillation) that the numeric solution of the reaction-diffusion equation becomes practically impossible. On the other hand, the points should be close enough to the bifurcation for the complex Ginzburg-Landau equation to apply to a reasonably good approximation.

One way, by which one can estimate a reasonable choice for the distance from the bifurcation, is to study how well the Stuart-Landau equation, approximates the true limit cycle solution for the homogeneous chemical reaction system. The Stuart-Landau equation is simply the complex Ginzburg-Landau equation without the diffusion term, *i.e.*

$$\frac{\partial W}{\partial \tau} = \lambda_2 W - g|W|^2 W. \quad (15)$$

If we put  $W = R e^{i\theta}$ , then Eq. (15) has the following simple solution

$$R = \sqrt{\frac{\sigma_2}{g'}}, \quad (16a)$$

$$\theta(\tau) = (\omega_2 - \sigma_2 \frac{g''}{g'})\tau, \quad (16b)$$

for the motion on the limit cycle. Expressing the solution in terms of the real time  $t$  we find that the Stuart-Landau prediction of the oscillations of the chemical concentrations will be described by the expression

$$\mathbf{c}(t) = \mathbf{c}_s + \epsilon \frac{\sigma_2}{g'} \left( e^{i\omega(\mu)t} \mathbf{U}_+ + e^{-i\omega(\mu)t} \overline{\mathbf{U}_+} \right), \quad (17)$$

where  $\omega(\mu) = \omega_0 + (\omega_2 - \sigma_2 \frac{g''}{g'})\mu$ . By plotting and comparing Eq. (17) together with the actual solution of the reaction system, one normally will get an initial estimation of whether or not the Ginzburg-Landau approach can be justified.

As the first point of investigation, we have chosen  $[\text{BrO}_3^-] = 0.01205 \text{ M}$  with  $[\text{H}^+] = 1 \text{ M}$ , which lies on the stable side of the Benjamin-Feir boundary ( $1 + \alpha\beta = 0.76$ ). Plots of the Stuart-Landau solution and the actual solution to the homogeneous Oregonator model are presented in Fig. 4a. The point is chosen at a distance from the bifurcation where the amplitude of the Stuart-Landau

solution is 10% of the value of  $[\text{Ce}^{4+}]$  at the stationary point  $\mathbf{c}_s$ . The results for the reaction-diffusion equation and the CGLE on a two-dimensional spatial domain are shown in Fig. 5. One clearly sees that the spatial wavelengths of the spirals are in excellent agreement, 4.3195 cm and 4.3194 cm respectively, determined by Fourier transformation. The amplitudes (not shown) also agree. Note also that the actual times it takes for the two spirals to evolve are almost the same, which clearly justifies the time scaling  $\tau = \mu t$  predicted by the Ginzburg-Landau theory.

In order to see what happens when the distance from the bifurcation point is increased, we have chosen two different values of  $[\text{BrO}_3^-]$  which give rise to amplitudes of 50% and 60% of the stationary concentration of  $\text{Ce}^{4+}$ . The comparisons for the homogeneous systems, *i.e.* between the actual limit cycle and the Stuart-Landau prediction are shown in Figs. 4b and 4c. The results of the integration of the reaction-diffusion system and the CGLE for these two working points are presented in Figs. 6a and 6b. From Fig. 6a it is evident at such large value of the bifurcation parameter  $[\text{BrO}_3^-] = 1.2950 \times 10^{-2}$  M, that the spiral center in the reaction-diffusion system no longer is localized in the center of the grid. This “symmetry break” is associated with the no-flux boundary conditions and we shall ignore it in our comparisons. Even though the complex Ginzburg-Landau equation fails in detail, it still reproduces the behavior of the reaction-diffusion system quite well. The spatial wavelengths are almost equal, 0.772 cm for the reaction-diffusion equation and 0.720 cm for the CGLE, and the characteristic time scales of spiral development are essentially the same for the two systems.

We now consider the case  $[\text{BrO}_3^-] = 1.3596 \times 10^{-2}$  M with an amplitude 60% of the average value for the homogeneous Stuart-Landau solution. From Fig. 6b we clearly see that at this rather large distance from the bifurcation point, the Ginzburg-Landau approach breaks down. The CGLE description predicts a stable spiral solution for the reaction-diffusion system, which itself exhibits a totally different pattern: A small spiral tip is formed near the boundary. After a few windings the spiral becomes unable to maintain its structure. It becomes unstable and breaks up into a large number of small spiral cores distributed throughout the spatial domain of the system. The visual appearance of the solution to the reaction-diffusion equation does indeed look “complex”. However, the system is not chaotic. This has been investigated by calculating the largest Lyapunov exponent  $\lambda_{\max}$  which is zero. The system is thus characterized by an oscillatory state which in this case is dominated by a large collection of relatively small spirals. Even though the resemblance between the reaction-diffusion system and the CGLE seems to be lost completely for this particular situation, one should note that the spatial wavelength of the small reaction-diffusion spirals still are in good agreement with the spatial wavelength found in the single spiral wave solution to the CGLE.

We now turn to a point on the bifurcation curve where the Benjamin-Feir parameter  $1 + \alpha\beta$  is negative, *viz.*  $[\text{BrO}_3^-]_{\text{Hopf}} = 0.073$  M and  $[\text{H}^+]_{\text{Hopf}} = 0.348$  M where the Benjamin-Feir parameter equals  $1 + \alpha\beta = -0.13$ . The actual integrations of the reaction-diffusion system were carried out at  $[\text{BrO}_3^-] = 0.0817$  M with  $[\text{H}^+] = [\text{H}^+]_{\text{Hopf}}$ . Here the Stuart-Landau amplitude is 10% of the average  $\text{Ce}^{4+}$  concentration, see Fig. 4d. The results for the reaction-diffusion equation and the CGLE are shown in Figs. 7a (phase) and 7b (amplitude). In both simulations (RDE and CGLE) we see that initially a spiral wave begins to develop from the center of the region. However, when two spiral windings have been formed, the spiral becomes unstable and a shock-like circular wave develops from the spiral core. When this shock wave hits the boundaries of the spatial domain a number of new spiral cores are generated (these are often referred to as phaseless points). Some of these phaseless points will repeat the scenario just described, whereas others will be annihilated either at the boundaries of the system or by colliding with other phaseless points. Finally, we end up with a spatio-temporally chaotic state which is totally dominated by phaseless points. From Fig. 7a and 7b we note the striking similarity between the behavior of the reaction-



diffusion equation and the corresponding CGLE. The development of the chaotic state takes place in almost the same time in the two systems. Furthermore, we see that the number of phaseless points in the spatial domain of the two systems are of the same order of magnitude. The chaotic character of the system is illustrated in Fig. 8, where the estimate of the largest Lyapunov exponent for the CGLE system,  $\lambda_{\max}$ , is plotted as a function of time. For  $t \rightarrow \infty$  the curve converges to a limiting value, the actual value of the Lyapunov exponent. As is evident from Fig. 8, the Lyapunov exponent is positive corresponding to chaotic dynamics.

The characteristic parameters used for the numerical integrations discussed in this section are summarized in table 3.

## 5 Computational details

The computation of the Hopf bifurcation diagram and the limit cycle solutions to the homogeneous Oregonator model were done with the bifurcation analysis package *CONT* [Schreiber 1995]. All integrations of the reaction-diffusion systems were performed on a CRAY92-computer using an explicit fourth order Runge-Kutta algorithm [Press *et al.* 1992]. The integration of the CGLE were done on a HPUX-workstation using the implicit Adams method from ODE-PACK [Hindmarsh 1983]. All integrations were carried out with no-flux boundary conditions and initial conditions chosen as described in [Kuramoto 1984, p. 106]. The Lyapunov exponent was computed by using a numerical approach described by Marek and Schreiber [1991].

## 6 Discussion

We consider two ways of using the complex Ginzburg-Landau equation for chemical reaction diffusion systems. One is to simplify calculations with models. Another one is to base realistic modelling of actual reaction diffusion systems on the CGLE with parameters determined directly by experiments performed on homogeneous systems [Hynne & Sørensen, 1993].

The numerical simplification of the reaction-diffusion models by the CGLE is obtained in two ways. First, the CGLE effectively reduces the dimension of the state space to two, which saves computation time, particularly for high-dimensional models. For example, calculation of waves for the big model of Györgyi *et al.* [1990] with its 26-dimensional state space, is no more difficult numerically than for any other model — once the Ginzburg-Landau parameters have been calculated. (Here the main problem is to obtain all the relevant diffusion coefficients). Second and most importantly, the use of the CGLE solves the problem (with the RDE) of the critical slowing down of pattern development that occurs near a bifurcation. The CGLE works with amplitudes, and the major effect of the time oscillations is accounted for analytically (in the transformation to the amplitude equation) rather than numerically. In fact, the critical slowing down has been completely scaled away in the CGLE. The importance of this feature can be appreciated by the significant reductions (by factors up to 1000) of the number of steps necessary for the integration, see table 3. In practice this means that the CGLE-calculation can be made with a work station whereas a supercomputer may be needed for integrating the RDE. In addition, the CGLE provides the solution in the form of a time and space dependent complex amplitude. This form is very convenient for understanding solutions, and it can easily be transformed back to actual time and space dependent concentrations of the (multitude of) species participating in the reactions.

The other way of using the CGLE for chemical systems is to set up the Ginzburg-Landau equation *directly* from experimental measurements on the corresponding *homogeneous* reaction system

using independently measured diffusion coefficients. It has been shown previously [Hynne & Sørensen 1993] how the parameters can be obtained from quenching experiments [Sørensen & Hynne 1989; Hynne *et al.* 1990; Vukojević *et al.* 1993; Nagy *et al.* 1995]. Thus, it is possible to model waves and chaos in real spatial systems without knowing the detailed mechanism of the chemical reactions.

The previous discussion shows that the Ginzburg-Landau approach to chemical reaction-diffusion systems is potentially very important. However, the use of the CGLE depends on the validity of the approximation for any particular system and operating point.

To throw some light on the question of the validity of the complex Ginzburg-Landau approximation we have compared solutions to a model reaction-diffusion system with their CGLE-approximations. For a chemical reaction diffusion system based on the Oregonator model of the Belousov-Zhabotinsky reaction, we find that there exist substantial regions for which the CGLE provides an excellent description of the dynamical behavior. This conclusion applies to parameter regions where the solutions show spatio-temporal chaos as well as regions with stable spiral waves. In the latter case, we demonstrate how the CGLE approximation eventually fails beyond a certain limit.

Experimentally, it is difficult to work too close to a Hopf bifurcation because small amplitude waves are difficult to detect and because of slow pattern evolution (critical slowing down). We conclude from the present study that one can reasonably expect a Ginzburg-Landau description to remain applicable to a system at experimentally feasible distances from the bifurcation point, provided the properties of the Oregonator model can be regarded as representative of the investigated system.

One condition for using the conclusions of the present study is that the real parts of the eigenvalues of the Jacobian matrix (other than the bifurcating pair) are sufficiently negative as in the Oregonator model considered here so that excitations out of the plane of oscillations decay fast. We are currently studying what happens when one such "transient mode" is slow, and the present work serves as a preliminary to that study as well as a prerequisite to using the CGLE with experiments and models.

To conclude, waves and spatio-temporal chaos in real chemical systems can be described by a complex Ginzburg-Landau equation with parameters  $\alpha$  and  $\beta$  determined by quenching experiments performed on the specific reaction at the specific point of operation used. The paper has demonstrated that, typically, the Ginzburg-Landau description will apply in a sufficiently wide region surrounding the bifurcation set to make the description useful in practice.

## References

- Allesie, M. A., Bonke, F. I. M. & Schopman, F. G. J. [1977] "Circus movement in rabbit atrial muscle as a mechanism of *tachycardia*," *Circ. Res* **41**, 9–18.
- Aranson, I. S., Kramer, L. & Weber, A. [1993] "Theory of interaction and bound states of spiral waves in oscillatory media," *Phys. Rev. E* **47**(5), 3231–3241.
- Coullet, P., Frisch, T., Gilli, J. M. & Rica, S. [1994] "Excitability in liquid crystals," *Chaos* **4**(3), 485–489.
- Cross, M. C. & Hohenberg, P. C. [1993] "Pattern formation outside of equilibrium," *Rev. Mod. Phys* **65**(3), 851–1112.
- Field, R. J. & Försterling, H.-D. [1986] "On the oxybromine chemistry rate constants with cerium ions in the Field-Körös-Noyes mechanism of the Belousov-Zhabotinsky reaction," *J. Phys. Chem* **90**, 5400.
- Field, R. J., Körös, E. & Noyes, R. M. [1972] "Oscillations in chemical systems. Thorough analysis of temporal oscillations in the bromate-cerium-malonic acid system," *J. Amer. Chem. Soc* **94**, 8649–8664.
- Field, R. J. & Noyes, R. M. [1974] "Oscillations in chemical systems IV. Limit cycle behavior in a model of a real chemical reaction," *J. Chem. Phys* **60**, 1877–1884.
- Györgyi, L., Turányi, T. & Field, R. J. [1990] "Mechanistic details of the oscillatory Belousov-Zhabotinsky reaction," *J. Phys. Chem* **94**, 7162–7170.
- Hindmarsh, A. C. [1983] "ODEPACK, a systematized collection of ODE solvers," in *Scientific Computing*, ed. R S Stepleman *et al.* (North-Holland, Amsterdam) pp. 55–64.
- Huber, G., Alstrøm, P. & Bohr, T. [1992] "Nucleation and transients at the onset of vortex turbulence," *Phys. Rev. Lett* **69**(16), 2380–2383.
- Hynne, F. & Sørensen, P. G. [1993] "Experimental determination of Ginzburg-Landau parameters for reaction-diffusion systems," *Phys. Rev. E* **48**(5), 4106–4109.
- Hynne, F., Sørensen, P. G. & Nielsen, K. [1990] "Quenching of chemical oscillations: General theory," *J. Chem. Phys* **92**, 1747.
- Kosek, J., Sørensen, P. G., Marek, M. & Hynne, F. [1994] "Normal form analysis of the Belousov-Zhabotinsky reaction close to a Hopf bifurcation," *J. Phys. Chem* **98**, 6128–6135.
- Kuramoto, Y. [1984] *Chemical Oscillations Waves and Turbulence* (Springer-Verlag, Berlin).
- Marek, M. & Schreiber, I. [1991] *Chaotic Behavior of Deterministic Dissipative Systems* (Academia, Prague).
- Nagy, A., Sørensen, P. G. & Hynne, F. [1995] "Quenching of oscillations in the permanganate-hydroxylamine reaction," *Z. Phys. Chem* **189**, 131–138.
- Newell, P. C. [1983] "Attraction and adhesion in the slime mold *Dictyostelium*," in *Fungal Differentiation: A Contemporary Synthesis*, ed. Smith, J. E. (Marcel Dekker, New York), vol. 43 of *Mycology Series* pp. 43–71.

- Nicolis, G. [1995] *Introduction to Nonlinear Science* (Cambridge University Press, Cambridge).
- Nielsen, K., Hynne, F. & Sørensen, P. G. [1991] “Hopf bifurcation in chemical kinetics,” *J. Chem. Phys* **94**, 1020–1029.
- Ouyang, Q. & Flesselles, J.-M. [1996] “Transition from spirals to defect turbulence driven by a convective instability,” *Nature* **379**, 143–146.
- Press, W. H., Teukolsky, S. A., Vetterling, W. T. & Flannery, B. P. [1992] *Numerical Recipes in C* (Cambridge University Press, New York), 2nd edn.
- Schreiber, I. [1995] *CONT — A Program for Construction of Parameter Dependence of Stationary or Periodic Solutions of Ordinary Differential or Difference Equations*, Department of Chemical Engineering, Prague Institute of Chemical Technology.
- Sørensen, P. G. & Hynne, F. [1989] “Amplitude & phases of small-amplitude Belousov-Zhabotinsky oscillations derived from quenching experiments,” *J. Phys. Chem* **93**, 5467–5474.
- Tyson, J. J. [1985] “A quantitative account of oscillations, bistability and travelling waves in the Belousov-Zhabotinskii reaction,” in *Oscillation and Travelling Waves in Chemical Systems*, eds. Field, R. J. & Burger, M. (Wiley-Interscience, New York) Chap. 3.
- Vukojević, V., Sørensen, P. G. & Hynne, F. [1993] “Quenching analysis of the Briggs-Rauscher reaction,” *J. Phys. Chem* **97**, 4091–4100.
- Zhabotinsky, A. M. [1991] “A history of chemical oscillations and waves,” *Chaos* **1**(4), 379–386.

## Captions of tables and figures

**Table 1:** Rate constants  $k_1, \dots, k_5$ , stoichiometric factor  $f$  and diffusion constants  $D_X, D_Y$  and  $D_Z$  used in the numerical integration of the Oregonator model, Eq. (14). The values of  $k_1, \dots, k_4$  are from Field and Försterling [1986],  $k_5$  and  $f$  from Nielsen *et al.* [1991] and diffusion constants from Hynne & Sørensen [1993]. (M = mol dm<sup>-3</sup>).

**Table 2:** Parameter values of the complex Ginzburg-Landau equation at the two points of the  $(1 + \alpha\beta)$ -curve plotted in Fig. 3 corresponding to the values of the two-parameter point  $([\text{BrO}_3^-]_{\text{Hopf}}, [\text{H}^+]_{\text{Hopf}})$ . The values of  $[\text{BrO}_3^-]$  actually used in the numerical integration of the reaction-diffusion system are given in table 3. Note that these values are off the bifurcation curve. The number  $\omega_0$  is the frequency of the sinusoidal oscillations exactly at the Hopf bifurcation point, whereas  $\sigma_2$  and  $\omega_2$  are the derivatives of the real and imaginary parts of the eigenvalue  $\lambda$  with respect to the bifurcation parameter (*i.e.*  $[\text{BrO}_3^-]$  for this particular example). The parameters  $g$  and  $d$  are the coefficients of the nonlinear term and the diffusion term in the complex Ginzburg-Landau equation, from which the dimensionless parameters  $\alpha$  and  $\beta$  are calculated (see Eqs. (6) and (10)). The Benjamin-Feir parameter  $1 + \alpha\beta$  for the two Hopf bifurcation points have been selected in order to study two different situations: At the first point ( $1 + \alpha\beta > 0$ ) we find that the reaction-diffusion system to admits of stable spiral wave solutions, whereas for the second point ( $1 + \alpha\beta < 0$ ) we find chaotic behavior.

**Table 3:** Integration parameters for the reaction-diffusion equation and the corresponding complex Ginzburg-Landau equation for different amplitudes relative to the stationary  $\text{Ce}^{4+}$  concentration and for the two selected points on the Hopf bifurcation curve (Fig. 1). The table shows the final integration time,  $t_{\text{end}}$ , and size,  $(r_x, r_y)$ , of the 2-dimensional domain for the specific bifurcation point distances of  $[\text{BrO}_3^-]$  used in the integration of the reaction-diffusion system.  $\tau_{\text{end}}$  and  $(s_x, s_y)$  indicate the corresponding scaled values used in the integration of the CGLE. The size of the grid is also shown together with a comparison between the steps used by the solver to reach  $t_{\text{end}}$  for the reaction-diffusion system and the associated CGLE (equal grid sizes was chosen for the integration of a specific reaction-diffusion system and the corresponding CGLE).

**Figure 1:** Bifurcation diagram showing the locations of Hopf bifurcations in the Oregonator model in the plane of the two parameters  $[\text{BrO}_3^-]$  and  $[\text{H}^+]$ . At a specific point  $[\text{BrO}_3^-] = 0.269$  M and  $[\text{H}^+] = 0.176$  M, the Hopf bifurcation changes stability from supercritical to subcritical corresponding to the solid and dashed curves respectively. For each point on the solid curve, a unique Ginzburg-Landau equation is defined, since the Ginzburg-Landau parameters  $\omega_2, \sigma_2, g$  and  $d$  can be calculated from Eqs. (7)–(9). The comparisons between the reaction-diffusion system and the complex Ginzburg-Landau equation have been carried out at the two points indicated on the curve.

**Figure 2:** (a): The dimensionless diffusion parameter  $\alpha$  along the supercritical branch in Fig. 1, plotted as a function of the parameter  $[\text{BrO}_3^-]$ . (b): Variation of the dimensionless parameter  $\beta$  associated with the nonlinear term in the complex Ginzburg-Landau equation along the supercritical branch in Fig. 1 plotted as a function of the parameter  $[\text{BrO}_3^-]$ .

**Figure 3:** The figure shows the variation of the Benjamin-Feir stability parameter  $1 + \alpha\beta$  along the curve of Hopf bifurcation points in the Oregonator model with  $[\text{BrO}_3^-]$  (a) and  $[\text{H}^+]$  (b) as parameter. From (a) and (b) we see that the Oregonator reaction-diffusion system crosses the Benjamin-Feir instability border at the point  $[\text{BrO}_3^-] = 0.073$  M and  $[\text{H}^+] = 0.348$  M where  $1 + \alpha\beta$  changes sign. As reference for further numerical investigations we have chosen two points

indicated on figure (a) and (b) with a filled and an open circle: One point showing stable spiral wave solutions and one point exhibiting spatio-temporally chaotic behavior.

**Figure 4:** Comparisons of the actual periodic solutions to the homogeneous Oregonator model (solid lines) and its approximation by the Stuart-Landau equation (dashed lines) at various distances from the bifurcation point. (a)-(c): Periodic solutions with amplitudes of 10%, 50% and 60% of the stationary concentration of  $\text{Ce}^{4+}$  at the Hopf bifurcation point represented in Fig. 1 with a filled circle. (d): Oscillations with an amplitude of 10% of the stationary concentration of  $\text{Ce}^{4+}$  associated with the Hopf bifurcation point represented with an open circle in Fig. 1.

**Figure 5:** The phase  $\phi$  of the oscillations for a stable spiral solution to the Oregonator reaction-diffusion system (RDE) and the associated complex Ginzburg-Landau equation (CGLE). The parameters used in the integrations correspond to the point marked with a filled circle in Figs. 1 and 3. In this case there is a very good agreement between the time scale under which the two patterns develop as well as the spatial wavelength of the two spirals. The numbers below each of the six snapshots of the RDE shows the time elapsed for that particular state in the RDE in units of  $10^5$  s. The corresponding snapshots for the CGLE are made at corresponding scaled times. The reaction-diffusion system has been solved for the parameter value  $[\text{BrO}_3^-] = 1.2051 \times 10^{-2}$  M corresponding to an amplitude of 10% of the stationary concentration of  $\text{Ce}^{4+}$  for the homogeneous Oregonator system.

**Figure 6:** Deviations between the reaction-diffusion system and the CGLE description become more evident when a larger distance from the bifurcation point is chosen. The figure compares the two systems at two finite distances corresponding to an amplitude of 50% (a) and 60% (b) of the stationary  $\text{Ce}^{4+}$  concentration. Due to nonlinear effects which become dominating as the distance increases the spiral moves away from the center of the domain and freezes at a point close to the boundary of the domain. In (a) the general characteristics (spatial wavelength and time of evolution) of the spirals in the two systems are still in good agreement. When the distance is increased further (b) the resemblance between the reaction-diffusion system and the CGLE is completely lost. The final state of the reaction-diffusion system is characterized by a number of small spirals distributed throughout the domain of the system. However, the spatial wavelength of these spirals are still described well by the CGLE.

**Figure 7:** Development of a chaotic state in the Oregonator reaction-diffusion system (RDE) and the associated complex Ginzburg-Landau equation (CGLE) represented by the phase  $\phi$  (a) and the amplitude (b) of the oscillations of  $[\text{Ce}^{4+}]$ . The characteristic parameter values used in the RDE and the CGLE correspond to the parameter point marked with an open circle in Figs. 1 and 3 where the Benjamin-Feir parameter satisfies  $1 + \alpha\beta < 0$ . Indications below the twelve snapshots of the RDE shows the evolution time for that particular state in the RDE as well as for the equivalent state in the CGLE measured in units of  $10^5$  s. Initially a spiral is formed at the center of the grid, but after approximately two windings have been, formed this structure breaks down being replaced by a set of phaseless points. (A phaseless point appears as a very localized dark spot on the  $[\text{Ce}^{4+}]$ -plot). The phaseless points will either split into other phaseless points or be annihilated at the boundary of the spatial domain. This scenario is then repeated, resulting in a very complicated interaction between the phaseless points. Finally a spatio-temporally chaotic state is reached in both the RDE and the CGLE. In the plots of the phase and the amplitude of  $[\text{Ce}^{4+}]$  we see a striking similarity between the behavior exhibited by the RDE and the CGLE. The two patterns develop in an almost synchronized manner. Even when the spiral is fully destroyed ( $t = 2.5 \times 10^5$  s) the positions of the phaseless points are still very similar in the corresponding RDE and CGLE states. The synchronization

is however lost at the final chaotic state, due to the fact that this chaotic state is characterized by a critical dependence on the initial conditions. The reaction-diffusion system has been solved for the parameter value  $[\text{BrO}_3^-] = 8.1935 \times 10^{-2}$  M corresponding to an amplitude of 10% of the stationary  $\text{Ce}^{4+}$  concentration.

**Figure 8:** Largest Lyapunov exponent,  $\lambda_{\max}$ , calculated for the complex Ginzburg-Landau equation for the state presented in Fig. 7 (shown in Figs. 1 and 3 with an open circle). The value of  $\lambda_{\max}$  is plotted as a function of time for a point where  $1 + \alpha\beta < 0$  giving rise to spatio-temporal chaos and a positive Lyapunov exponent. In this sense, the state of the system can be characterized as chaotic.

<i>Constant</i>	<i>Value</i>
$k_1/\text{M}^{-3}\text{s}^{-1}$	2.0
$k_2/\text{M}^{-2}\text{s}^{-1}$	$3.0 \times 10^6$
$k_3/\text{M}^{-1}\text{s}^{-1}$	$3.0 \times 10^3$
$k_4/\text{M}^{-2}\text{s}^{-1}$	42.0
$k_5/\text{s}^{-1}$	0.167
$f$	0.7905
$D_X/\text{cm}^2\text{s}^{-1}$	$1.0 \times 10^{-5}$
$D_Y/\text{cm}^2\text{s}^{-1}$	$1.6 \times 10^{-5}$
$D_Z/\text{cm}^2\text{s}^{-1}$	$0.6 \times 10^{-5}$

Table 1:

<i>Parameter</i>	<i>Spiral</i>	<i>Turbulence</i>
$[\text{BrO}_3^-]_{\text{Hopf}}/\text{M}$	$1.2014 \times 10^{-2}$	$8.1765 \times 10^{-2}$
$[\text{H}^+]_{\text{Hopf}}/\text{M}$	1.0000	$3.2721 \times 10^{-1}$
$\omega_0/\text{s}^{-1}$	0.1085	0.1200
$\sigma_2/\text{s}^{-1}$	3.4468	0.6000
$\omega_2/\text{s}^{-1}$	5.3686	0.8196
$g/10^{13}\text{M}^{-2}\text{s}^{-1}$	$4.08 + i3.62$	$6.54 + i2.02$
$d/10^{-5}\text{cm}^2\text{s}^{-1}$	$1.01 - i0.28$	$1.03 - i0.38$
$\alpha$	-0.2712	-0.3651
$\beta$	0.8846	3.1020
$1 + \alpha\beta$	0.76010	-0.13237

Table 2:



<i>amplitude deviation</i>	<i>Spiral</i>			<i>Turbulence</i>
	10%	50%	60%	10%
$[\text{BrO}_3^-]/\text{M}$	$1.2051 \times 10^{-2}$	$1.2950 \times 10^{-2}$	$1.3596 \times 10^{-2}$	$8.1765 \times 10^{-2}$
$(\mu - \mu_0)/\text{M}$	$3.7456 \times 10^{-5}$	$9.3642 \times 10^{-4}$	$1.3484 \times 10^{-3}$	$1.7082 \times 10^{-4}$
$t_{\text{end}}/10^3\text{s}$	6.50	0.96	0.44	3.30
$\tau_{\text{end}}$	24.3	89.9	59.3	56.4
$(r_x, r_y)/\text{cm}$	(30.0, 30.0)	(10.0, 10.0)	(5.0, 5.0)	(20.0, 20.0)
$(s_x, s_y)$	(0.184, 0.184)	(0.306, 0.306)	(0.198, 0.198)	(0.261, 0.261)
grid	128x128	256x256	256x256	128x128
steps - RDE/CGLE	$6.5 \times 10^5/649$	$1.9 \times 10^5/9600$	$8.8 \times 10^4/3747$	$3.3 \times 10^5/3300$

**Table 3:**

**Figure 1:**

**Figure 2:**

**Figure 3:**

**Figure 4:**

**Figure 5:**

**Figure 6:**

**Figure 6:**

**Figure 7:**

**Figure 7:**

**Figure 8:**